PNAS
www.pnas.org

Supplementary Information for:

Microglia depletion exacerbates demyelination and impairs remyelination in a neurotropic coronavirus infection

[1]Alan Sariol, [2]Samantha Mackin, [1]Merri-Grace Allred, [4]Chen Ma, [4]Yu Zhou, [4]Qinran Zhang [4]Xiufen Zou, [5]Juan E. Abrahante, [3]David K. Meyerholz, and [1,2]Stanley Perlman

[1]Interdisciplinary Program in Immunology, Departments of [2]Microbiology and Immunology and [3]Pathology, University of Iowa, Iowa City, IA 52242

[4]School of Mathematics and Statistics, Wuhan University, Wuhan, China, 430072

[5]University of Minnesota Informatics Institute (UMII), Minneapolis, MN, USA

Corresponding author:

Stanley Perlman, M.D., Ph.D., Department of Microbiology and Immunology, BSB 3-712, University of Iowa, Iowa City, IA 52242, tele: 319-335-8549; FAX: 319-335-9006; email: Stanley-perlman@uiowa.edu.

This PDF file includes:

Supplementary materials and methods
Figures S1 to S2
SI References

www.pnas.org/cgi/doi/10.1073/pnas.2007814117

SI Materials and Methods

Isolation of immune cells from brain and spinal cord. Mice were sacrificed and perfused with PBS at indicated days p.i. Brains and spinal cords were harvested and mechanically diced and digested with 1 mg/ml collagenase D (Roche) and 0.1 mg/ml DNase I (Roche) at 37°C for 30 minutes. Digested tissue was passed through a 70µm cell strainer and subsequently centrifuged in a 37% Percoll gradient. Pelleted cells were then washed and resuspended in culture media for further use in flow cytometric analysis or cell sorting.

Antibodies and flow cytometry. The following antibodies were used for flow cytometry in this study: CD45-PE-Cy7 (clone 30-F11; BioLegend); CD11b-eFluor 450 (clone M1/70; eBioscience); Ly6G-APC, -PE (clone 1A8, Biolegend); Ly6C-PerCP-Cy5.5, -APC (clone HK1.4; eBioscience); MHCII (IA/IE), -PerCP-eFluor710 (clone M5/114.15.2; eBioscience); MHCI (H-2Kb/H2-Db), -APC/Fire 750 (clone 28-8-6; Biolegend); CD16/CD32-PerCP-Cy5.5 (2.4G2; BD Biosciences); CD3-BV510 (clone 17A2, Biolegend); CD3e-APC, -PerCP-Cy5.5 (clone 145-2C11, Biolegend); CD4-eFluor 450, -PerCP-Cy5.5, -APC (clone RM4-5; eBioscience); CD8a-e450, -PE, -APC (clone 53-6.7; eBioscience); IFN-γ-PerCP-Cy5.5, -FITC (clone XMG1.2; eBioscience); FOXP3-FITC (clone FJK-16s; eBioscience); and CD11c-FITC (clone HL3; BD Biosciences). Data were acquired using a FACSVerse (BD Biosciences) and analyzed using FlowJo software (Tree Star). Cells were sorted using a FACSAria Fusion or FACSAria II (BD Biosciences).

RNA extraction, qPCR, and primers. Mice were sacrificed and perfused with PBS at indicated days p.i. Brains and spinal cords were manually homogenized in TRIzol reagent (Thermo Fisher Scientific) and RNA extracted according to manufacturer instructions. Separately, monocytes/macrophages ($CD45^{hi}CD11b^{+}Ly6G^{-}$) were FACS-sorted from spinal cords as described above and RNA was extracted using an RNeasy Micro Kit (Qiagen), per manufacturer instructions. RNA was transcribed into cDNA using Moloney murine leukemia virus reverse transcriptase (M-MLV Reverse Transcriptase, Thermo Fisher Scientific). Expression levels were determined by quantitative PCR (qPCR) using a Quantstudio 3 Real-Time PCR system and PowerUp Sybr Green reagents (Applied Biosystems). Expression levels were normalized to those of hypoxanthine-guanine phosphoribosyltransferase (HPRT) and presented as $2^{-\Delta Ct}$, where ΔCt = Ct of gene of interest – Ct of *Hprt*. The following primer sets were used:

Gene Name	Forward	Reverse
ApoE	CTGACAGGATGCCTAGCC	TCCCAGGGTTGGTTGCTTTG
Axl	GGAGGAGCCTGAGGACAAAGC	ACAGCATCTTGAAGCCAGAGTAGG
Clec7a	GACTTCAGCACTCAAGACATCC	TTGTGTCGCCAAAATGCTAGG
CXCL12	TGCATCAAGTGACGGTAAACCA	CACAGTTTGGAGTGTTGAGGAT
MHV gRNA	AGGGAGTTTGACCTTGTTCAG	ATAATGCACCTGTCATCCTCG
HPRT	GCGTCGTGATTAGCGATGATG	CTCGAGCAAGTCTTTCAGTCC
IGF1	CCGAGGGGCTTTTACTTCAACAA	CGGAAGCAACACTCATCCACAA
Lgals3	TTGAAGCTGACCACTTCAAGGTT	AGGTTCTTCATCCGATGGTTGT
Tgm2	GAAGGAACACGGCTGTCAGCAA	GATGAGCAGGTTGCTGTTCTGG

Viral plaque assay. Mice were sacrificed and perfused with PBS. Brains and spinal cords were harvested and manually homogenized in PBS and frozen. Frozen samples were then thawed and centrifuged to pellet cells and tissue. Virus titers in the resulting supernatants were determined by plaque assay of HeLa-MHVR cells, as previously described (1).

Quantification of demyelination, vacuolization, and cellular debris. Following PBS perfusion, spinal cords were harvested and bisected in the mid-sagittal plane, then fixed in zinc formalin. Fixed spinal cords were then embedded in paraffin and 8µm sections were cut in the sagittal plane and stained with Solvent blue 38 (Sigma-Aldrich), also known as Luxol fast blue (LFB), and counterstained with Harris hematoxylin (Leica) and Eosin Y (Sigma-Aldrich) for visualization of demyelinating lesions and infiltrating cells. Sections were then imaged using an Olympus BX61 light microscope and demyelination quantified by tracing both demyelinating lesions and total white matter in ImageJ software (NIH). Percent demyelination was then calculated as a ratio of the total area of demyelinating lesions over total white matter area for each spinal cord.

For quantification of vacuolization and cellular debris, LFB and H&E-stained sections were examined using a post-examination method of masking the pathologist to tissue group assignments (2). Tissues were evaluated for degeneration changes, and in these regions, clear spaced vacuolization (both number and size) and extent of cellular debris (i.e. pyknotic nuclear debris) were both evaluated per 400x field (i.e., 0.058917 mm^2 per 400x field).

Intracellular cytokine and transcription factor staining. Immune cells were isolated from spinal cords as described above, then stimulated with JHMV-specific M133 or S510

peptide (Bio-synthesis Inc., Genscript) in complete RPMI 1640 media (Gibco) in the presence of GolgiPlug (1µg/ml, BD Biosciences) and antigen-presenting cells (CHB3 cells, B cell line, H-2D^b, I-A^b) for 6 hours at 37°C. The M133 and S510 peptides encompasses residues 133–147 of the transmembrane (M) protein, and residues 510–518 of the surface (S) glycoprotein and are the immunodominant CD4 and CD8 T cell epitopes, respectively (3–5). These peptides were used at a final concentration of 5 µM (M133) or 1 µM (S510). BD Cytofix/Cytoperm and Perm/Wash buffers (BD Biosciences) were used for cell fixation/permeabilization and subsequent staining for intracellular cytokines. For Foxp3 staining, an eBioscience Foxp3 / Transcription Factor Staining Buffer Set was used for fixation/permeabilization and subsequent staining.

RNA-Seq and gene expression profiling of microglia. Microglia (CD45^{int} CD11b$^+$) were sorted from isolated immune cells of spinal cords at the indicated days p.i. RNA was isolated using an RNeasy Micro Kit (Qiagen) according to manufacturer's instructions. Subsequent library preparation and sequencing was performed at the University of Minnesota Genomics Center.

RNA isolates were quantified using a fluorimetric RiboGreen assay and RNA integrity was assessed using capillary electrophoresis (Agilent BioAnalyzer 2100) to generate an RNA integrity number (RIN). Samples with RIN values above 2-3 and at least 250 pg total RNA were then used to generate sequencing libraries using a SMARTer Stranded Total RNA-Seq v2 – Pico Mammalian kit (Takara Bio). Briefly, between 250pg-10ng of total RNA were fragmented and then reverse transcribed into cDNA using random primers, with a template switching oligo incorporated during cDNA synthesis to allow for full length cDNA synthesis and retain strand specificity. Illumina sequencing adapters and barcodes were then added to the cDNA by PCR, followed by cleavage of ribosomal cDNA. Uncleaved fragments were then enriched by PCR for 12-16 cycles. Final library size distribution was again validated using capillary electrophoresis and quantified using fluorimetry (PicoGreen). Indexed libraries were then normalized and pooled for sequencing.

Libraries were then loaded onto a NextSeq 550 (single read, Illumina) cartridge, where clustering occurred on-board the instrument. After clustering, sequencing was commenced using Illumina's 2-color SBS chemistry. Following sequencing, Base call (.bcl) files for each cycle of sequencing were generated by Illumina Real Time Analysis software. Primary analysis and de-multiplexing were performed using Illumina's CASAVA

software 1.8.2. The end result of the CASAVA workflow was de-multiplexed FASTQ files for subsequent analysis.

75bp FastQ single-end reads (19.7-25.9 million reads per sample) were trimmed using Trimmomatic (version 0.33) enabled with the optional "-q" option; 3bp sliding-window trimming from 3' end required minimum Q30. Quality control of raw sequence data for each sample was performed using FastQC. Read mapping was performed via Hisat2 (v2.1.0) using the mouse genome (mm10) as reference. Gene quantification was performed using Feature Counts for raw read counts. Differentially expressed genes were identified using the edgeR (negative binomial) feature in CLCGWB (Qiagen) using raw read counts. We filtered the generated list on the basis of a minimum 2 absolute fold change after $\log_2$ transformation and an FDR corrected p value < 0.05. Heat maps of both total and selected differentially expressed genes were generated using Heatmapper software (6). Complete RNA-Seq data were deposited in the NCBI's Gene Expression Omnibus (GEO) database (GSE144911).

Electron microscopy and toluidine blue staining. Mice were sacrificed and perfused with PBS at 21 dpi. Spinal cords were removed and fixed in 2.5% glutaraldehyde with 0.1M sodium cacodylate. Samples were then postfixed in in 1% osmium tetroxide, stained in 2.5% uranyl acetate, and dehydrated and embedded in Epon resin. Sections were cut on a Leica EM UC6 ultramicrotome to 80nm thickness for toluidine blue staining or 8nm and mounted on copper slot grids for use in transmission electron microscopy. Sections were stained with toluidine blue and mounted on slides for subsequent visualization on an Olympus BX61 microscope. Sections on slot grids were then contrasted with 5% uranyl acetate and Reynold's lead citrate. Electron micrographs were obtained on a Hitachi HT7800 transmission electron microscope.

Axon measurement and g-ratio calculation. Inner axon diameter, total myelinated axon diameter, and myelin thickness were measured using ImageJ software on electron micrographs. g-ratios were calculated as (inner axon diameter/total myelinated axon diameter). g-ratios were displayed both independently and as a function of inner axon diameter. Myelin thickness was displayed both independently and as a function of inner axon diameter.

157 *Immunofluorescence*. Following sacrifice and perfusion at indicated days p.i., spinal cords
158 were fixed in 4% paraformaldehyde, followed by immersion in 10%, 20%, and 30%
159 sucrose solutions for cryoprotection. Samples were frozen by heat displacement and cut
160 to 8µm thickness on a Leica Microm cryostat. Sections were then immersed in PBS with
161 0.1% Triton-X (Sigma-Aldrich), incubated in CAS block (Thermo Fisher Scientific), and
162 incubated with a 1:500 dilution of rabbit anti-Olig2 polyclonal antibody (Millipore) at 4°C in
163 a humidity chamber overnight. Sections were stained with a 1:200 dilution of Alexa Fluor
164 Plus 488 goat-anti-rabbit secondary antibody (Thermo Fisher Scientific) for one hour prior
165 to mounting with Vectashield Antifade Reagent (Vectashield Laboratories) and imaging
166 with an Olympus BX61 microscope. $Olig2^+$ cells were manually counted using ImageJ
167 software (NIH) and displayed as a ratio of cells per area of counting in mm^2.
168 *Statistics*: Data are presented as the mean ± SEM. Mann-Whitney *U* test were used to
169 analyze differences between groups. P values of less than .05 were considered significant.
170 *P<0.05, **$P<0.01$, ***$P<0.001$, ****P<0.0001.

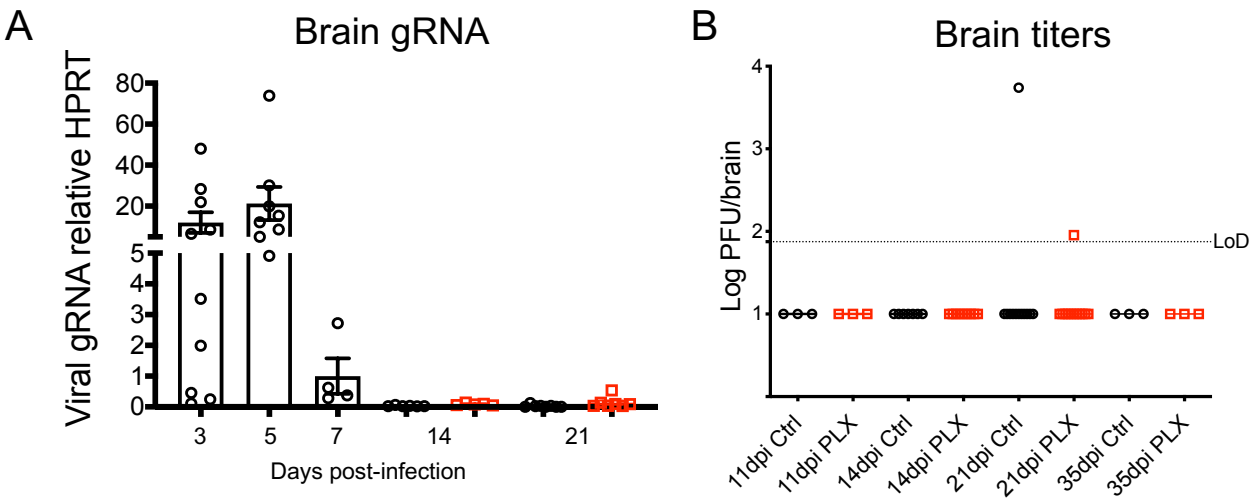

Supplemental Figure S1: Virus is cleared in the brain beginning at 7 dpi. Mice were infected intracranially with 700 PFU JHMV, then fed at day 7 p.i. with PLX5622-containing or control chow. Expression levels of viral genomic RNA as assessed by qPCR (**A**) (n=4-10 mice/group) and infectious virus titers as determined by plaque assay (**B**) (n=3-12 mice/group) in the brain.

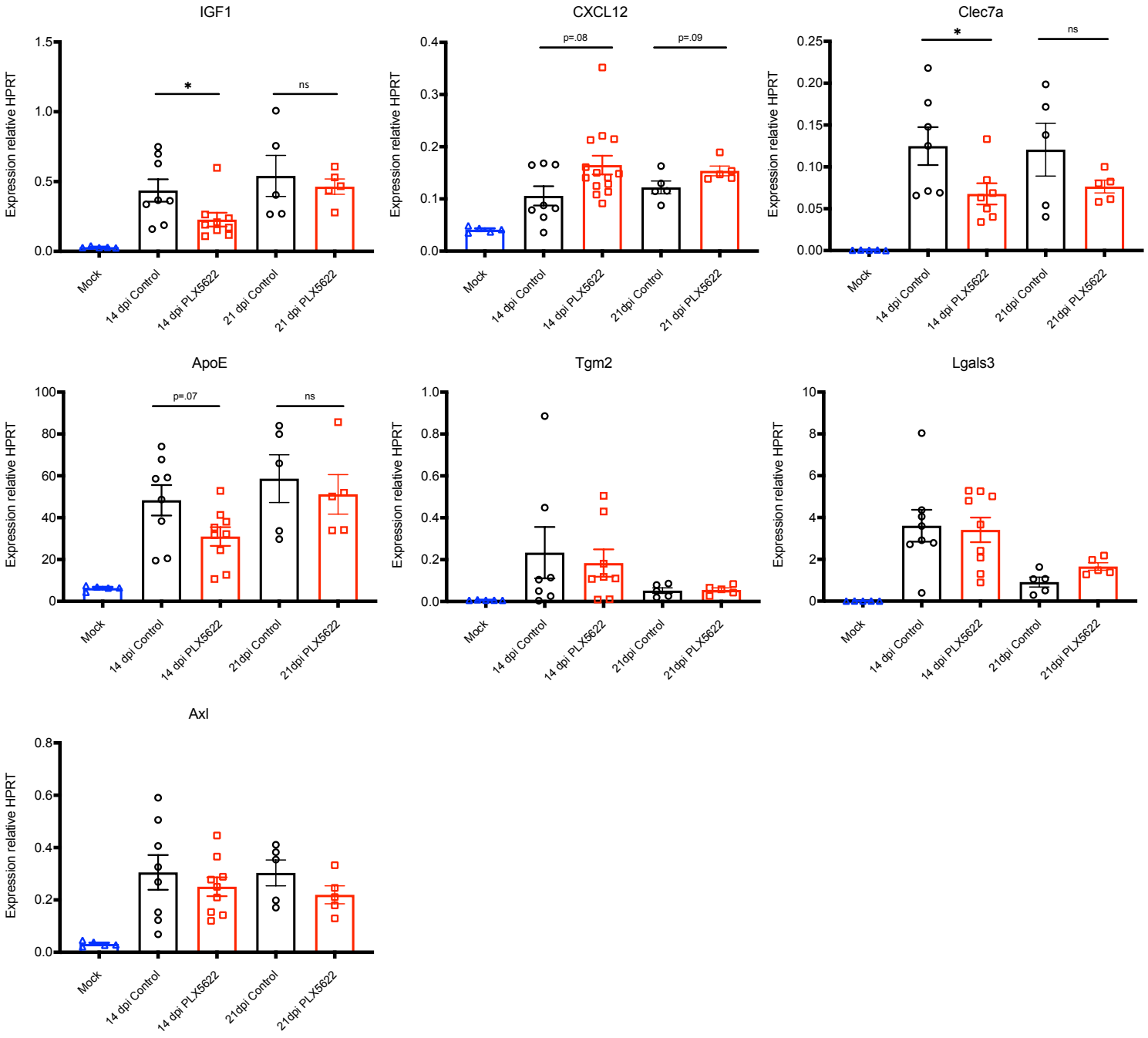

Supplemental Figure S2: qPCR of genes involved in remyelination and debris clearance in whole spinal cord. Infected mice were treated at day 7 p.i. with PLX5622-containing or control feed. Spinal cords were analyzed for indicated mRNA transcripts by qPCR at 14 and 21 dpi, as well as following mock infection. Data are representative of 5-9 mice per group and represent the mean ± SEM, **P*<.05, by Mann-Whitney *U* test.

SI References

1. L. D. Eckerle, *et al.*, Infidelity of SARS-CoV Nsp14-exonuclease mutant virus replication is revealed by complete genome sequencing. *PLoS Pathog.* **6**, e1000896 (2010).

2. D. K. Meyerholz, A. P. Beck, Principles and approaches for reproducible scoring of tissue stains in research. *Lab. Investig. J. Tech. Methods Pathol.* **98**, 844–855 (2018).

3. S. Xue, A. Jaszewski, S. Perlman, Identification of a CD4+ T cell epitope within the M protein of a neurotropic coronavirus. *Virology* **208**, 173–179 (1995).

4. R. F. Castro, S. Perlman, CD8+ T-cell epitopes within the surface glycoprotein of a neurotropic coronavirus and correlation with pathogenicity. *J. Virol.* **69**, 8127–8131 (1995).

5. C. C. Bergmann, Q. Yao, M. Lin, S. A. Stohlman, The JHM strain of mouse hepatitis virus induces a spike protein-specific Db-restricted cytotoxic T cell response. *J. Gen. Virol.* **77**, 315–325 (1996).

6. S. Babicki, *et al.*, Heatmapper: web-enabled heat mapping for all. *Nucleic Acids Res.* **44**, W147-153 (2016).